



Assessment the Effect of Irrigation and Plant Cover Pattern on Land Surface Temperature Using Remote Sensing

Mahmoud, A. K.¹, A. M. El-Gindy² and T. M. H. Yossif³

¹Soil Physics and Chemistry Dept., Desert Research Centre, Cairo, Egypt.

²Agricultural Engineering Dept. Faculty of Desert Agriculture, King Salman International University.

³Pedology Dept., Desert Research Centre, Cairo, Egypt.

Amr_73@yahoo.com

Abstract: Winter wheat is a vital crop in Egypt. Moreover water status is an essential for irrigation planning especially at different plant cover pattern which affected by different parameters such as leaf area index (LAI) and plant height. Further; A few crop water indicators, such as leaf equivalent water thickness (EWT) and canopy water content (CWC) plus Land surface temperature (LST) have been estimated using remote sensing techniques for different stage of winter wheat growth. This study focus on relation between the (LST) and previous parameters particularly with total water applied (TWA), (CWC), (LAI) and vapour pressure deficit (VPD) at Ismailia governorate for wheat crop. Thus; study used Landsat 8 Operational Land Imager (OLI), Band 4, 5, 6, 7 and 10 with 30m spatial resolution covering the study area and taken on different dates 10/11/2020, 26/11/2020, 28/12/2020 and 29/01/2021, were obtained from the USGS (2020 and 2021). The result revealed that there are a positive reaction and relation between both (CWC – EWT) and (TWA) where by increasing water applied the (CWC) and the (EWT) increased. For instance; (CWC) and (EWT) obtained a highest value (459.4 g.m⁻² and 0.43 g.cm⁻²) respectively after irrigated by a high amount of water (12.25 m³.day⁻¹.fed⁻¹). Data represented that land surface temperature (LST) changed during measuring date from highest value (27.9C°) to lowest value (17.3C°) which effected by wheat stage and increasing on plant height. Further; the highest values for (LAI) has recorded (1.07m².m⁻²) with plant height (63cm) comparing with (43cm) which obtained (0.8 m².m⁻²) for (LAI). Notably; when plant height increased from (20cm to 43 cm) the value of deferent between air temperature (T_{air}) and (LST) was recorded (3.4 C and 3.9 C°) respectively. Moreover; there is a significant linear relation between (LST) and (VPD); where by increasing (LST) the (VPD) increase which reflect that plant suffering and has a water stress. Thus; (VPD) can estimated by knowing (LST) value by using this model ($VPD = 0.119 (LST) - 1.2102$) with R²= 0.9203. Finally; the flowing regression model was developed by utilized some parameters (CWC), (VPD) and (LST) to determine amount of water for different wheat stages in the Ismailia governorate in sandy soil with R²= 0.831. $TWA = 0.0187(CWC) - 0.93(VPD) - 0.4826 (LST) + 11.72$.

[Mahmoud, A. K., A. M. El-Gindy and T. M. H. Yossif. **Assessment the Effect of Irrigation and Plant Cover Pattern on Land Surface Temperature Using Remote Sensing** *Nat Sci* 2022; 20(1):35-46]. ISSN 1545-0740 (print); ISSN 2375-7167 (online). <http://www.sciencepub.net/nature>. 4.doi:[10.7537/marsnsj200122.04](https://doi.org/10.7537/marsnsj200122.04).

Key words: Crop water content, Land surface temperature, Leaf area index, Leaf equivalent water thickness, Remote sensing, Total water applied and Vapour pressure deficit

1. Introduction

Land Surface Temperature (LST) is often a direct control on herbaceous plants but has been underappreciated on the alpine grassland phenology in response to climate change. Although the way in which vegetation phenology mediates the feedback of vegetation to climate systems is now well understood, the magnitude of these changes is still unknown. A thorough understanding of how the recent shift in phenology may impact on. In addition, the air temperature has a major influence on plant growth (Gill *et al.*, 2015). During the past few decades, sprawling investigations have revealed a deep mechanistic understanding of vegetation phenology

variations in response to temperature based on plant physiological processes (Lin *et al.*, 2018).

Notable, that land cover composition had a relatively stable correlation with LST at different scales, and that most area-related landscape configuration metrics could be replaced by land cover composition (Lin *et al.*, 2018). In another study, where the two were compared, land cover composition was seen to be more important in determining LST than land cover configuration, although configuration had a significant effect when composition was kept constant (Zhou *et al.*, 2011). Among the land cover variables, percent cover and

density of plant especially Leaf Area Index (LAI) had the most influence.

Leaf area index (LAI), which is defined as “one half of the total green leaf area per unit horizontal ground surface area” (Chen and Black, 1992), is used for the study of vegetation dynamics and as an input to many climate models (Yan *et al.*, 2012). LAI can be estimated from the field or by using remote sensing data. Even though direct and indirect estimations of LAI (Gower *et al.*, 1999) are the most accurate, field measurements can be extremely time-consuming and labour intensive (Jonckheere *et al.*, 2004). Remote sensing provides interesting opportunities for the estimation of LAI over large spatial and temporal scales. Although the remote sensing models require field-estimated LAI for calibration and validation (Asner *et al.*, 2003), the estimates from remote sensing make LAI quite significant for the assessments of vegetation dynamics (Turner *et al.*, 1999) and climate change. Moreover, Remote sensing has made it possible to study temperature variations across large areas and the factors influencing them (Voogt and Oke, 2003). Land surface temperature (LST), which has a large influence on air temperature, can be estimated using thermal imagery. Further, Remote sensing techniques can be used to effectively monitor and diagnose vegetation water conditions, accurately reflect physiological status of vegetation under water stress, rapidly recognize drought, and immediately adopt irrigation measures (Wang *et al.*, 2013 and Zhang *et al.*, 2012).

Memorable; the commonly used physiological indicators to assess plant water conditions mainly include stomata conductance, leaf water potential (Zhou *et al.*, 2013), canopy water content (CWC) (Clevers *et al.*, 2010) and leaf equivalent water thickness (EWT) (Jacquemoud *et al.*, 1996). (EWT), defined as quantity of water per unit leaf area, is more relevant to the water absorption of incoming radiation. Additionally, EWT plays a crucial role in biogeochemical processes such as photosynthesis, evaporation, and primary productivity (Running and Gower, 1991). Its rapid decreases or shortage is an important early stress indicator. CWC, expressed as the quantity of water per unit area of ground surface, is widely utilized to monitor vegetation water conditions (Clevers *et al.*, 2008) and is determined not only by vegetation water status but also by crop growth and development stages (Zhang and Zhou, 2015). Moreover, an atmospheric vapour pressure deficiency (VPD) has much influence on water used by plants (Braunworth

and Mack, 1989). Where, Vapour Pressure Deficit dictates how efficiently a plant might balance its internal energy with that of the wider environment. (Gardner and Shock, 1989) suggested that AVPD in the range of 1-6 kPa is necessary to define a baseline that could be used in many locations.

On the other hand, Wheat is the vital strategic crop not only for all countries but also for Egypt. Wheat is considerable an essential staple food of about 36% of the world population. Hence, expanding wheat productivity, from each unit of water and soil, has becomes an exigency. However, by sacristry of water, studies should focus on irrigation water management for Wheat to acquire a highest production with low amount of irrigation water without creating any stresses whatever on soil or crop.

Finally, agricultural drought mainly reflects soil water status as well as crop growth and morphology, which can be used to reflect the degree of soil water deficit to crop water demand. Thus, the relation among factors of agricultural system especially Land Surface Temperature (LST), irrigation water, vapour pressure deficit (VPD), Crop Water Content (CWC), leaf Equivalent Water Thickness (EWT) and Leaf Area Index (LAI) should be controlled to get a positive upshot. Consequently, the aim of this study is monitoring and determining the irrigation water for winter Wheat using remote sensing depending on several items such as Land Surface Temperature (LST), Vapour Pressure Deficit (VPD), Crop Water Content (CWC) and Leaf Area Index (LAI) for Wheat. Finally, create a simple mathematic relation between to quantify the total water applied for wheat per day.

2. Material and methods

Experimental location

The experimental was carried out at Seraphim - Ismailia governorate; throw the project “Wastewater reuses in the MENA region - Addressing the challenges Direct Treated Wastewater Reuse Model for Planting Wheat, Barley and Cotton; which located in north eastern of Egypt (30° 28' 49.14"N - 32° 13' 29.86"E). The study has established in 10 November of 2019 to 29 January 2021 during the season of the winter Wheat. Ismailia site is about 30 m above sea level with an average rainfall of 28.2 mm, temperatures of 16.8 °C, relative humidity of 64.03%, and wind speed of 2.86 m/s (Table 1). These Meteorological parameters are derived from the NASA's MERRA-2 (2020 – 2021).

Table 1. Climatic characteristics at Ismailia governorate. (2020-2021)

Month	Prc.*	Tem.	Tem. min	Tem max	Hum.	Sun shine	Wind (2m)	ET _o
	mm/m	°C	°C	°C	%	%	m/s	mm/d
2020								
Nov	19.3	19.3	14.24	24.4	63.5	76.7	2.8	3.02
Dec	5	16.4	10.8	22.1	65.1	65.5	2.7	3.0
2021								
Jan	3.9	14.9	9.0	20.8	63.5	68.1	3.1	2.8

*Prc. = Precipitation; Tem. min/max = minimum/maximum temperature; Hum. = relative humidity; Sun shine = day length; Wind (2m) = wind speed at 2m; ET_o = Reference Evapotranspiration.

The soil of experimental is sandy texture, none saline, and none calcareous. Silt and clay content; average 3.9% and 4.7%, respectively for Ismailia soils. Field capacity and available water are very low 5.6%, and 4.5% with EC in soil equal to

1.37dS.m⁻¹. Winter Wheat was cultivated on 23 November 2020 by using a drip irrigation system (built-in line) (GR 4L/50cm/h – 1.2bar) and distance between lines 0.6m (Fig., 1).



Figure1. Drip irrigation system with built-in line dripper for irrigating winter Wheat.

Hence, water requirement for Wheat calculated according to Allen *et al.* (1998) (Table 2) by the following Equations.

$$ET_c = ET_o * K_c \quad (1)$$

Where:

- ET_c Crop Evapotranspiration (mm.day⁻¹).
- ET_o Reference Evapotranspiration (mm.day⁻¹).
- K_c Crop coefficients.

$$IR_n = ET_c - P_{eff} \quad (2)$$

Where:

- IR_n Net irrigation requirement, (mm.day⁻¹).
- Et_c Crop evapotranspiration, (mm.day⁻¹).
- P_{eff} Effective rainfall, (mm.day⁻¹).

$$TWA = (IR_n/Ea) * 4.2 \quad (3)$$

Where:

- TWA Total Water Applied (m³.fed⁻¹.day⁻¹).
- IR_n Net irrigation requirement, (mm.day⁻¹).
- Ea Overall irrigation efficiency for modern irrigation system (drip), approximately 95%. d for surface irrigation is 65 – 75% (Phocaides, 2000).

Table 2. Total Water Applied (TWA) and crop coefficients (K_c) for winter wheat during measurement.

Item	Nov.	Dec.	Jan.
Days*	8	31	31
K _c	0.7	0.9	1.15
TWA	4.7	7.14	12.25

*Days=from cultivated wheat; K_c=Crop coefficients; TWA=Total Water Applied (m³.fed⁻¹.day⁻¹)

Vapour Pressure Deficit (VPD)

The VPD metric consists of air temperature, leaf temperature, and relative humidity which measured in Kilopascals (Richard *et al.*, 2015) to get VPD, need to subtract an actual vapour pressure of the air (VP_{air}) from the saturated vapour pressure (VP_{sat}).

$$VPD = VP_{sat} - VP_{air} \quad (4)$$

To get (VP_{sat}), need to know the temperature of the saturated environment, in this case, the leaf of the plant by using an infrared temperature gun.(UNI-T UT300C, which is an infrared thermometer that is specially designed for surface temperature measurements within the range from -20 °C to 400 °C). The formula for VP_{sat} (in Kilopascals kPa) is:

$$VP_{sat} = \frac{610.7 * 10^{\left(\frac{7.5T}{237.3+T}\right)}}{1000} \quad (5)$$

Where: T is leaf Temperature in Celsius (°C)

To get (VP_{air}), need to know the temperature and humidity of the air. The formula for VP_{air} (in Kilopascals kPa) is:

$$VP_{air} = \frac{610.7 * 10^{\left(\frac{7.5T}{237.3+T}\right)}}{1000} * \frac{RH}{100} \quad (6)$$

Where:

T = Air Temperature in Celsius (°C).
RH = Relative Humidity (%).

Satellite images

Landsat 8 Operational Land Imager (OLI), Band 4, 5, 6, 7 and 10 with 30m spatial resolution covering the study area and taken on different dates 10/11/2020, 26/11/2020, 28/12/2020 and 29/01/2021, were obtained from the USGS (2020 and 2021). The

satellite images were used to calculate NDVI, LST, LAI, NDWI, NDII, and CWC (Fig., 2) as follow. The value extraction was performed using Arc GIS software (ESRI, 2017).

- a) Normalized Difference Vegetation Index (NDVI) which utilizes red and Near-Infrared (NIR) wavelengths, where chlorophyll reflects more NIR and green light at healthy and dense vegetation and vice versa. Equation (7), (Tucker, 1980), for the computation of NDVI is:

$$NDVI = \frac{NIR - RED}{NIR + RED} \quad (7)$$

Where:

NDVI = Normalized Difference Vegetation Index
NIR = Reflectance in the near infrared band, and
RED = Reflectance in the red band.

- b) Land Surface Temperature (LST) was calculated according to the following equations (Abdullah *et al.*, 2020).

$$L_{\lambda} = M_L * Q_{cal} + A_L \quad (8)$$

Where:

M_L = Band-specific multiplicative rescaling factor for band ten equal to 0.0003342.
Q_{cal} = Quantized and calibrated standard product pixel values (DN).
A_L = Band-specific additive rescaling factor equal to 0.1.
L_λ = Top of Atmosphere (TOA) spectral radiance (Watts. m⁻². srad⁻¹. μm⁻¹).

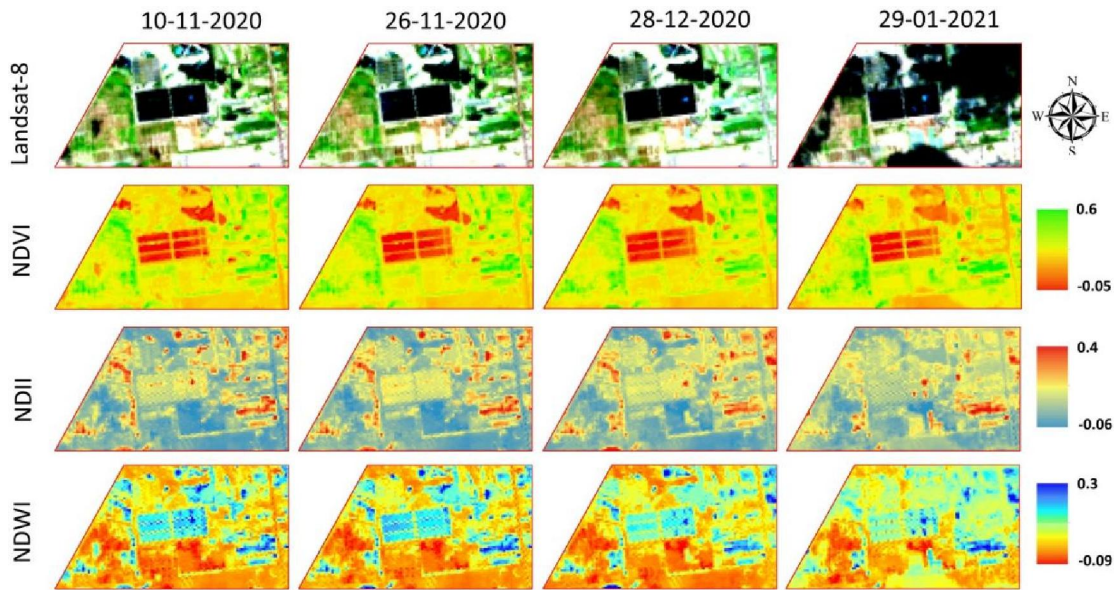


Figure 2. Spectral vegetation indices (NDVI, NDII and NDWI) calculated from Landsat-8 OLI image of the study area.

The following equation (9) was used to convert TOA to satellite brightness temperature for satellite sensor:

$$B_t = [K_2 / \ln(1 + K_1 / L_\lambda)] - 273.15 \quad (9)$$

Where:

K_1 & K_2 = Calibration constants that represent at-sensor spectral radiances (774.89 and 1321.07, respectively)

B_t = satellite Brightness temperature in °C

After that calculate emissivity and surface emissivity for the study area as follows:

$$PV = \left[\frac{NDVI - NDVI_{min}}{NDVI_{max} - NDVI_{min}} \right]^2 \quad (10)$$

$$E = 0.004 * PV + 0.986 \quad (11)$$

Where:

$NDVI_{min}$ = Minimum value of NDVI value.

$NDVI_{max}$ = Maximum value of NDVI value.

PV = Proportion of Vegetation.

E = Surface Emissivity.

Finally, land surface temperature was calculated using the following equation:

$$LST = B_t / (1 + [W * (B_t / 14380) * \ln(E)]) \quad (12)$$

Where:

W = Wavelength of emitted radiance equal to 10.895

LST = Land surface temperature °C.

c) Leaf Area Index (LAI) was calculated according to Saito *et al.* (2001).

$$LAI = 0.57 * \exp(2.33 * NDVI) \quad (13)$$

Where:

LAI = leaf area index ($m^2.m^{-2}$)

NDVI = Normalized Difference Vegetation Index

d) Crop Water Content (CWC) was calculated using flowing equations (Abdullah *et al.*, 2020 and Raymond *et al.*, 2018).

$$NDWI = \frac{B_{NIR} - B_{SWIR1}}{B_{NIR} + B_{SWIR1}} \quad (14)$$

$$NDII = \frac{B_{NIR} - B_{SWIR2}}{B_{NIR} + B_{SWIR2}} \quad (15)$$

$$CWC = 0.230 + 1.18 * NDII \quad (16)$$

Where:

NDWI = Normalized Difference Water Index

NDII = Normalized Difference Infrared Index

B_{NIR} & B_{SWIR1} = Near-Infrared (B5) and SWIR1 (B6) bands, respectively

B_{NIR} & B_{SWIR2} = Near-Infrared (B5) and SWIR2 (B7) bands, respectively

CWC = Crop water content ($kg.m^{-2}$)

e) Leaf equivalent water thickness (EWT, $g.cm^{-2}$) at the leaf level usually equals the leaf water content per unit leaf area (Danson *et al.*, 1992). Here, at the canopy level, EWT is defined as the ratio between the quantity of water and the area, otherwise known as crop water content per unit leaf area Equation (17).

$$EWT = \frac{CWC}{LAI} * 100 \quad (17)$$

Where:

EWT = Leaf equivalent Water Thickness ($g.cm^{-2}$)

LAI = Leaf Area Index ($m^2.m^{-2}$)

CWC = Crop Water Content ($g.m^{-2}$)

Statistical model

The simple regression models with predictor variables $X_1; \dots ; X_p$ can be describe by Equation (18).

$$y = B_0 + B_1X_1 + \dots + B_pX_p + k \quad (18)$$

Where: Variable y , called a response or dependent variable, depends on another variables $X_{(1..p)}$ which is called the independent or predictor variable (also called the regress or variable), B_0 is intercept, $B_{1..p}$ is the slope parameters and the variability of the error (k) is constant for all values of the repressor.

3. Result and Discussion

Crop water content and Leaf equivalent water thickness

Figures 3 and 4 illustrate that the crop water content (CWC) was changed during the different stage of wheat crop. In addition; CWC recorded (250.8 g.m^{-2}) at the first stage of wheat and after irrigated by ($7 \text{ m}^3.\text{day}^{-1}.\text{fed}^{-1}$). Moreover; after two months from cultivated wheat the CWC obtained a highest value (459.4 g.m^{-2}) after irrigated by a high amount of water ($12.25 \text{ m}^3.\text{day}^{-1}.\text{fed}^{-1}$). Data reflect that there is a positive reaction and relation between CWC and total water applied where by increasing water applied the CWC increase. This relation can explain by the flowing equation:

$$CWC = 207.89e^{TWA} \quad (19)$$

Where:

- CWC = Crop water content (g.m^{-2}).
- TWA = Total water applied ($\text{m}^3.\text{fed}^{-1}.\text{day}^{-1}$)

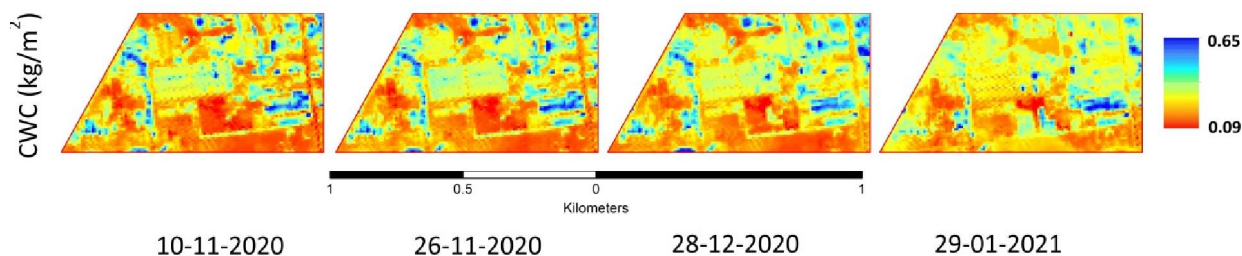


Figure 3. Crop water content (CWC) calculated from Landsat-8 OLI image of the study area.

Consequently, CWC is utilized to monitor vegetation water conditions (Clevers *et al.*, 2010) and (Clevers *et al.*, 2008) and is determined not only by vegetation water status but also by crop growth and development stages (Zhang and Zhou, 2015). On the other hand; Leaf equivalent water thickness (EWT) has a good relation with (TWA). DATA reflect the value of EWT increase by increasing TWA. For instance; EWT recorded 0.031 g.cm^{-2} when added amount of water ($4.7 \text{ m}^3.\text{fed}^{-1}.\text{day}^{-1}$), however, the highest value (0.43 g.cm^{-2}) for EWT obtained after irrigated by amount of water ($12.25 \text{ m}^3.\text{fed}^{-1}.\text{day}^{-1}$). So; EWT can used as parameter to reflect not only water content but also the amount of water which adding to irrigate crop because EWT plays a crucial role in biogeochemical processes such as photosynthesis, evaporation, and primary productivity (Running and Gower, 1991; Running and Nemani, 1991). Thus, the polynomial equation can used to estimate the EWT for wheat related to TWA.

$$EWT = 0.0021TWA - (8 * 10^{-5})(TWA)^2 + 0.029 \quad (20)$$

Where:

- EWT = Leaf equivalent water thickness (g.cm^{-2}).
- TWA = Total water applied ($\text{m}^3.\text{fed}^{-1}.\text{day}^{-1}$)

Finally, The CWC and EWT can be used as physiological indicators to water stress especially at a different stage for crop (Zhou *et al.*, 2013).

Plant height, Land surface temperature (LST) and leaf area index (LAI)

The Land Surface Temperature (LST) was changed during the measuring dates from highest value ($27.9 \text{ }^\circ\text{C}$) to lowest value ($17.3 \text{ }^\circ\text{C}$) (Fig., 5) which effected by growing stage and increasing on plant height. For instance, the value of LST was obtained at $21.6 \text{ }^\circ\text{C}$ with plant height equal 20cm, but after wheat growing and recorded 43cm the LST decrease to $16.6 \text{ }^\circ\text{C}$ (Fig., 6). Contrariwise, the value of LST increased to become $17.3 \text{ }^\circ\text{C}$ when wheat plant recorded 63cm as a plant height. Cao *et al.* (2010) found that LST decreased steadily with increasing mean vegetation height when height was less than 20m. Notably when plant height increased from 20 cm to 43 cm, the value of different between air temperature (T_{air}) and LST was recorded ($3.4 \text{ }^\circ\text{C}$ and $3.9 \text{ }^\circ\text{C}$), respectively. However;

by increasing the plant height to (63cm) the value of ($T_{air} - LST$) decrease dynamics to recorded (1.6 C°). Consequently, there is a significant relation between plant height and LST; also between plant height and ($T_{air} - LST$) the flowing formula (21 and 22) explain this relation:

$$LST = 0.004(PL)^2 - 0.427(PL) + 28.145 \quad (21)$$

$$T_{air} - LST = -0.0023(PL)^2 + 0.1442(PL) + 1.6507 \quad (22)$$

Where:

- LST = Land Surface Temperature (°C).
- PL = Plant height for wheat (cm).
- T_{air} = Air temperature (°C).

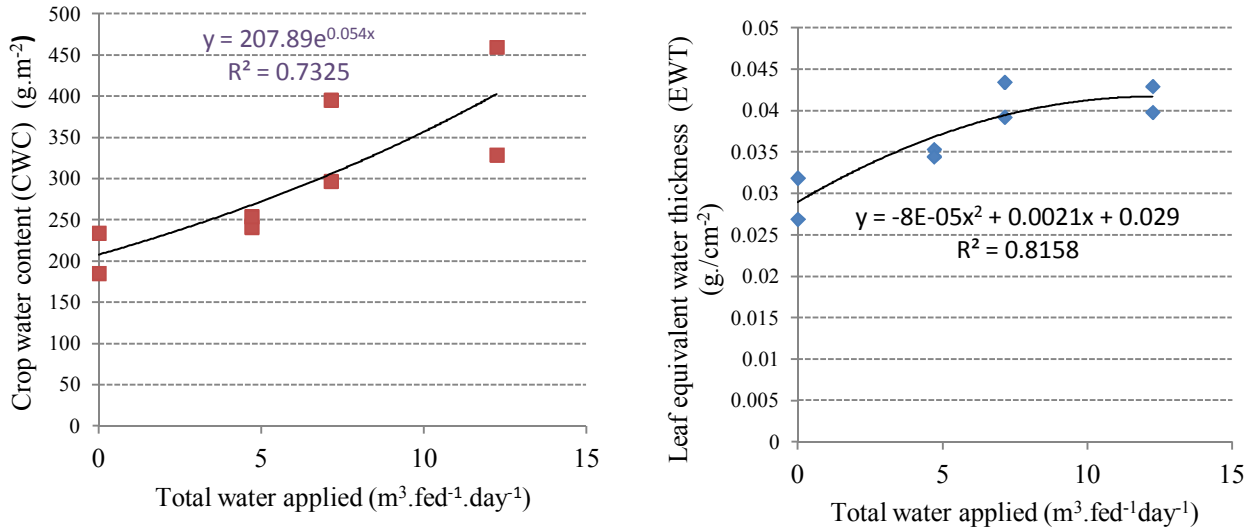


Figure 4. Impact total water applied on Crop Water Content (CWC) and leaf Equivalent Water Thickness (EWT).

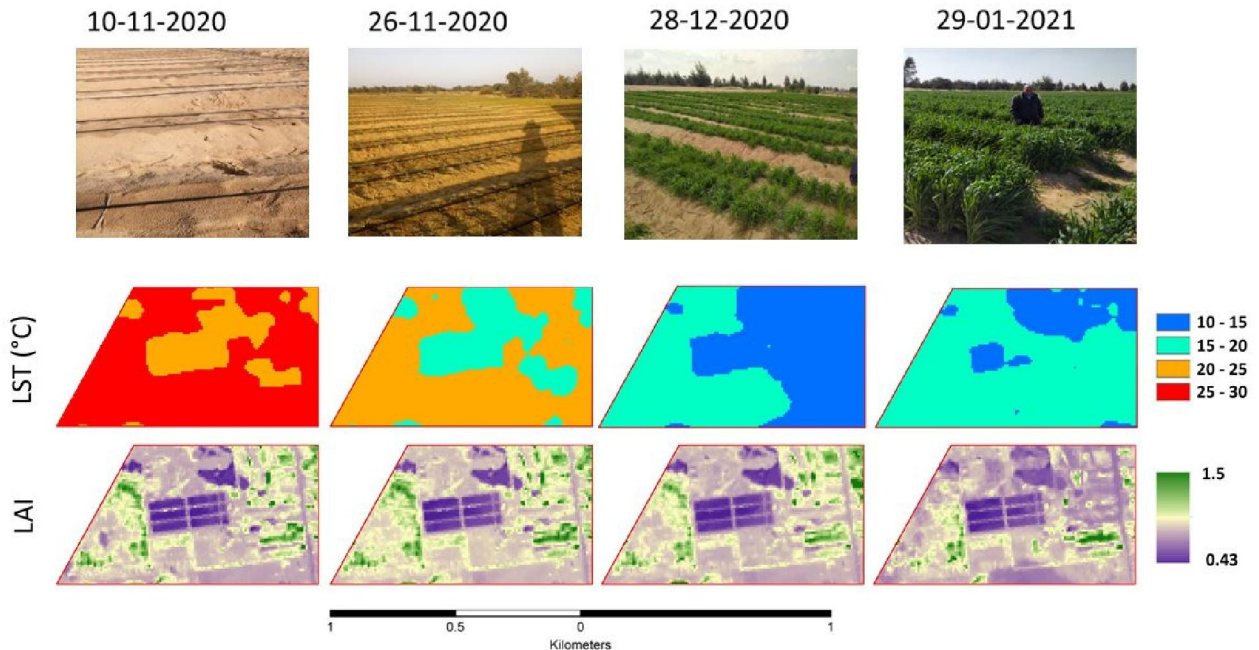


Figure 5. Land surface temperature (LST) and leaf area index (LAI) calculated from Landsat-8 OLI image of the study area

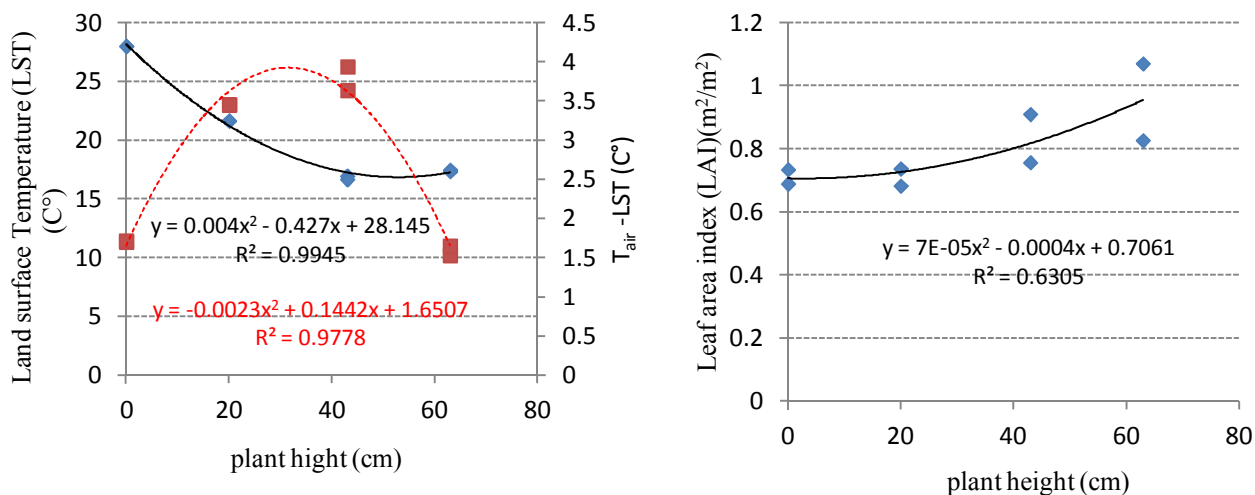


Figure 6. Influence of plant height on Land surface temperature (LST) and leaf area index (LAI)

As shown at fig. (6) Data represented that there are a variations on the values leaf area index (LAI) related to the different plant height (PL). For instance; the highest values for (LAI) has recorded ($1.07\text{m}^2.\text{m}^{-2}$) with plant height (63cm) comparing with (43cm) which obtained ($0.8\text{m}^2.\text{m}^{-2}$) for (LAI). Furthermore; after 11days from sowing date; the value of plant height was (20cm) and observed a lowest value for (LAI) by ($0.68\text{m}^2.\text{m}^{-2}$). Thus; the dynamics of plant height during the whole growing season could be used to assess critical genetic traits, fundamental plant physiology and environmental effects (Malambo *et al.*, 2018) Leaf Area Index (LAI) is an important physiological trait and can be used to indicate the performance of a plant canopy for growth and yield (Roth *et al.*, 2018). Obviously, on the basis of previous studies, LAI has been considered as one of the crucial factors which affect the plant metabolic activities through its effect on irrigation or fertigation management due to improper VPD and crop transpiration (Medrano *et al.*, 2005). There is a Dynamic response between both LAI and Plant Height (PL) for Wheat with R^2 more than 0.63, equation (23).

$$LAI = (7 * 10^{-5})(PL)^2 - 0.0004 (PL) + 0.7061 \quad (23)$$

Where:

LAI = Leaf Area Index.

PL = Plant height for wheat (cm).

Land Surface Temperature (LST) and Vapour Pressure Deficit (VPD).

Land surface temperature (LST) is a key variable in determination of the land surface energy budget, thus often assimilated into land surface models (Rodell *et al.*, 2004). LST (as soil or vegetation canopy temperature) is also used in models of vegetation stress. In addition; Vapour pressure deficit (VPD) has been widely recognized as the evaporative driving force for water transport, the potential to reduce plant water consumption and improve water productivity by regulating VPD. Consequently; data on fig (7) represent that there are a significant linear relation between LST and VPD where by increasing LST the VPD increase and reflect that plant suffering and has a water stress. In particular; data recorded a highest value for VPD by (2.233 KPa) when LST obtained (27.9C°) before cultivated wheat but after one month, on 28th December 2021, and irrigated plant with average ($7\text{m}^3.\text{fed}^{-1}.\text{day}^{-1}$) the VPD got (0.886 KPa) with reduced at LST value to acquired (16.9C°). Moreover; after two months especially on 29th January2021 the VPD recorded (0.934 KPa) with LST value (17.3 C°).

Subsequently; As the VPD increases, Evapotranspiration also increases as the air has an increased capacity to hold water vapour, creating a larger potential gradient across the leaf-air and soil-air boundaries (Garratt, 1992). Further; Vapour Pressure Deficit reflects plant efficiency and how to deal with internal energy balance and external environment. Thus; the VPD can estimated by

knowing LST value using the flowing model (24) which reflects this significant relation with $R^2=0.9203$:

$$VPD = 0.119(LST) - 1.2102 \quad (24)$$

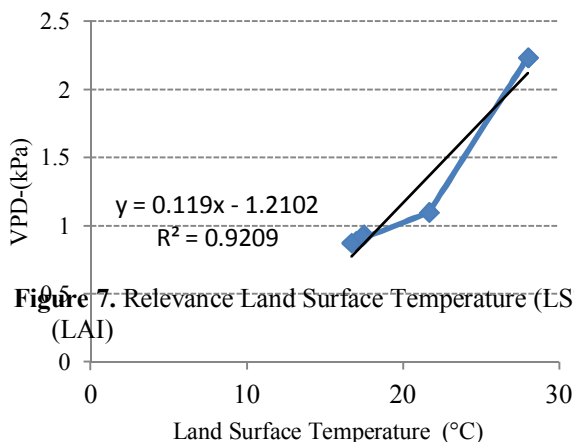
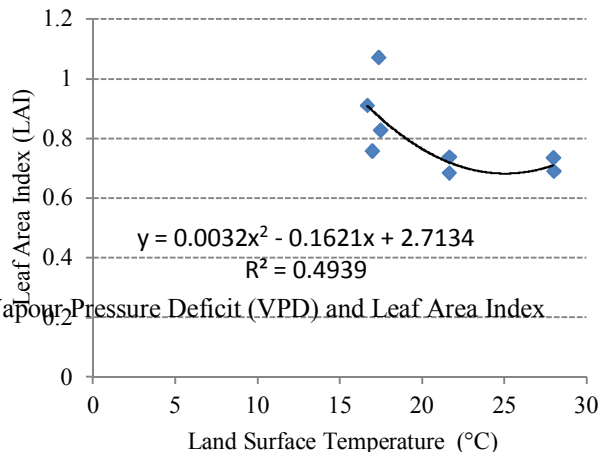


Figure 7. Relevance Land Surface Temperature (LST), Vapour Pressure Deficit (VPD) and Leaf Area Index (LAI)



On the other hand, Fig. (7) illustrate that Leaf Area Index (LAI) effected on land surface temperature (LST); for instance, when (LAI) obtained lowest value by $(0.68 \text{ m}^2.\text{m}^{-2})$ the (LST) recorded (21.6°C) . Further; after 60 days from cultivated wheat the value of (LST) decreased dynamics to acquired (17.3°C) with increasing at the (LAI) value by $(1.07 \text{ m}^2.\text{m}^{-2})$. obviously; that (LAI) has reverse relation with (LST) by increasing (LAI) the (LST) decrease because (Azad *et al.*, 2020) that the observed daytime cooling was due to increased Evapotranspiration, while night-time warming is found to increase with latitude and decrease with average rainfall. In addition; while LAI values fluctuated according to the vegetative period of the tree: highest in spring summer, with an average value of 2.3 and lower in autumn winter with an average of 1.38. The environmental variables showed a statistically significant relationship with respect to LAI, giving positive but weak correlations (Ibáñez *et al.*, 2021) Thus; (LAI) parameter reflect to plant height and density moreover (Lijun *et al.*, 2015) allowed us to disregard the impacts of different soil conditioners and application rates on the dynamic changes in the LAI of wheat. The flowing equation (25) explain the relation between (LAI) and (LST) but with weak correlation ($R^2=0.493$).

$$LAI = 0.0032(LST)^2 - 0.1621(LST) + 2.7134 \quad (25)$$

Where:
LAI = Leaf Area Index.

Where:-

VPD = Vapour Pressure Deficit (KPa).
LST = Land Surface Temperature ($^\circ\text{C}$).

LST = Land surface temperature ($^\circ\text{C}$).

Statistical model

A model is a schematic representation of the conception of a system or an act of mimicry or a set of equations, which represents the behaviour of a system (Murthy, 2003). A crop water content and plant growth model is a very effective tool for predicting the possible impacts of different factors on irrigation and crop growth. Total water applied models are useful for solving various practical problems in agriculture. Thus regression model (26) was developed by utilized some parameters CWC, VPD and LST to determine amount of water for different wheat stages in the Ismailia governorate in sandy soil.

$$TWA = 0.0187(CWC) - 0.93(VPD) - 0.4826(LST) + 11.72 \quad (26)$$

$$R^2= 0.831$$

TWA = Total water applied ($\text{m}^3.\text{fed}^{-1}.\text{day}^{-1}$)
CWC = Crop water content ($\text{g}.\text{cm}^{-2}$).
VPD = Vapour Pressure Deficit (KPa).
LST = Land surface temperature ($^\circ\text{C}$).

Conclusion

The direct impact of irrigation on the land surface is to enhance soil moisture, which in turn changes the surface albedo, and can have a subsequent influence on the solar radiation absorption (Rn). Irrigation has an indirect impact on vegetation,

which can affect ET. Irrigation can be expected to offer feedback to the surface climate, especially LST. Consequently, Data reflect that there is a positive reaction and relation between CWC and total water applied (TWA) where by increasing water applied the CWC increase. For instance; CWC obtained a highest value (459.4 g.m⁻²) after irrigated by a high amount of water (12.25 m³. fed⁻¹.day⁻¹). Leaf equivalent water thickness (EWT) EWT can used as parameter to reflect not only water content but also the amount of water which adding to irrigate crop using this model ($EWT = 0.0021TWA - (8 * 10^{-5})(TWA)^2 + 0.029$) .on the other hand; when plant height increased from (20cm to 43 cm) the value of deferent between air temperature (T_{air}) and land surface temperature (LST) was recorded (3.4 C and 3.9 C°) respectively. Further; the highest values for (LAI) has recorded (1.07m².m⁻²) with plant height (63cm) comparing with (43cm) which obtained (0.8 m².m⁻²) for (LAI). Moreover; there is a significant linear relation between LST and Vapour pressure deficit Vapour pressure deficit VPD where by increasing LST the VPD increase and reflect that plant suffering and has a water stress. Thus; VPD can estimated by knowing LST value by applied at this model $VPD = 0.119(LST) - 1.2102$. Finally; the flowing regression model was developed by utilized some parameters CWC, VPD and LST to determine amount of water for different wheat stages in the Ismailia governorate in sandy soil with R²= 0.831.. $TWA = 0.0187(CWC) - 0.93(VPD) - 0.4826(LST) + 11.72$

Acknowledgements

The author wishes to acknowledge the project “Wastewater reuse in the MENA region - Addressing the challenges Direct Treated Wastewater Reuse Model for Planting Wheat, Barley and Cotton” and their team work for excellent encouragement, technical and recommendations.

Reference

1. **Abdullah, H., Omar, D.K., Polat, N., Bilgili, A.V., Sharef, S.H. 2020.** A comparison between day and night land surface temperatures using acquired satellite thermal infrared data in a winter wheat field. Remote Sensing Applications: Society and Environment. 19 -100368, 1 - 9. <https://doi.org/10.1016/j.rsase.2020.100368>
2. **Allen, R.G., Pereira, L.S., Raes, D., Smith, M. 1998.** Crop evapotranspiration. Guidelines for computing crop water requirements. FAO irrigation and drainage paper No.56. FAO, Rome.
3. **Asner, G.P., Scurlock, J.M., Hicke, J.A. 2003.** Global synthesis of leaf area index observations: Implications for ecological and remote sensing studies. Glob. Ecol. Biogeogr. 12, 191–205.
4. **Azad Rasul, Sa’ad Ibrahim, Ajoke R. Onojeghuo, Heiko B. 2020.** A Trend Analysis of Leaf Area Index and Land Surface Temperature and Their Relationship from Global to Local Scale. Land. 9(10), 388. <https://doi.org/10.3390/land9100388>
5. **Braunworth, W.S. Jr., Mack, H.J. 1989.** The possible use of the crop water stress index as an indicator of Evapotranspiration deficits and yield reductions in sweet corn. J. Am. Soc. Hort. Sci. 114, 542-546.
6. **Cao, X., Onishi, A., Chen, J., Imura, H. 2010.** Quantifying the cool island intensity of urban parks using ASTER and IKONOS data. Landsc. Urban Plan. 96, 224–231. <https://doi.org/10.1016/j.landurbplan.2010.03.008>.
7. **Chen, J.M., Black, T.A. 1992.** Defining leaf area index for non-flat leaves. Plant Cell Environ. 15, 421–429.
8. **Clevers, J.G.P.W., Kooistra, L., Schaepman, M.E. 2008.** Using spectral information from the NIR water absorption features for the retrieval of canopy water content. Int. J. Appl. Earth Obs. 10:388–97.
9. **Clevers, J.G.P.W., Kooistra, L., Schaepman, M.E. 2010.** Estimating canopy water content using hyperspectral remote sensing data. Int. J. Appl. Earth Obs. 12:119–25.
10. **Danson, F.M., Steven, M.D., Malthus, T.J., Clark J.A. 1992.** High-spectral resolution data for determining leaf water content. Int J Remote Sens. 13:461–70.
11. **ESRI. 2017.** Arc GIS Spatial Analyst: Advanced-GIS Spatial Analysis Using Raster and vector data, ESRI, 380 New york, USA.
12. **Gardner, B.R., Shock, C.C. 1989.** Interpreting the crop water stress index. ASAE, 89, 2642.
13. **Garratt, J.R. 1992.** The Atmospheric Boundary Layer. Cambridge University Press, Cambridge, UK.
14. **Gill, A.L., Gallinat, A.S., Sanders-DeMott, R., Rigden, A. J., Short Gianotti, D. J., Mantooth, J. A., Templer, P. H. 2015.** Changes in autumn senescence in northern hemisphere deciduous trees: a metaanalysis of autumn phenology studies. Annals of Botany 116:875–888.

15. **Gower, S.T., Kucharik, C.J., Norman, J.M. 1999.** Direct and indirect estimation of leaf area index, fAPAR, and net primary production of terrestrial ecosystems. *Remote Sens. Environ.* 70, 29–51.
16. **Ibáñez, R., Ponce-Donoso, M., Vallejos-Barra, Ó. 2021.** The relation of leaf area index, temperatures and ultraviolet radiation in trees areas of a city in central Chile. *Scientia Forestalis*, 49(129), e3170. <https://doi.org/10.18671/scifor.v49n129.02>
17. **Jacquemoud, S., Ustin, S., Verdebout, J., Schmuck, G., Andreoli, G., Hosgood, B. 1996.** Estimating leaf biochemistry using the PROSPECT leaf optical properties model. *Remote Sens Environ.* 56:194–202.
18. **Jonckheere, I., Fleck, S., Nackaerts, K., Muys, B., Coppin, P., Weiss, M., Baret, F. 2004.** Review of methods for in situ leaf area index determination: Part I. Theories, sensors and hemispherical photography. *Agric. For. Meteorol.* 121, 19–35.
19. **Kjelgaard, J.F., Stockle, C.O., Evans, R.G. 1996.** Accuracy of canopy temperature energy balance for determining daily evapotranspiration. *Irrig. Sci.* 16, 149-157.
20. **Lijun Su, Quanjiu Wang, Chunxia Wang, Yuyang Shan. 2015.** Simulation Models of Leaf Area Index and Yield for Cotton Grown with Different Soil Conditioners. *PLOS ONE*. DOI:10.1371/journal.pone.0141835
21. **Lin, S., Shao, L., Hui, C., Sandhu, H.S., Fan, T., Zhang, L., Li, F., Ding, Y., Shi, P. 2018.** The effect of temperature on the developmental rates of seedling emergence and leaf-unfolding in two dwarf bamboo species. *Trees* 32:751–763.
22. **Malambo, L., Popescu, S.C., Murray, S.C., Putman, E., Pugh, N.A., Horne, D.W., Richardson, G., Sheridan, R., Rooney, 3 B., Avant, R., Vidrine, M., McCutchen, B., Baltensperger, D., Bishop, M. 2018.** Multitemporal Field-based Plant Height Estimation using 3D Point Clouds Generated from Small Unmanned Aerial Systems High-resolution Imagery, *International Journal of Applied Earth Observation and Geoinformation* 64: 31–42. <https://doi.org/10.1016/j.jag.2017.08.014>
23. **Medrano, E., Lorenzo, P., Sanchez-Guerrero, M.C., Montero, J.L. 2005.** Evaluation and modelling of greenhouse cucumber-crop transpiration under high and low radiation conditions. *Scientia Horticulturae*. 105(2):163–175. <https://doi.org/10.1016/j.scienta.2005.01.024>. [MERRA-2 \(NASA.gov\)](http://www.nasa.gov/merra-2).
24. **Murthy, V.R.K. 2003.** Crop growth modelling and its applications in agricultural meteorology. In: *Satellite Remote Sensing and GIS Applications in Agricultural Meteorology*, Proceedings of a Training Workshop, 7th–11th July 2003. Dehra Dun, India, pp. 235–261.
25. **Phocaides, A. 2000.** Technical Handbook on Pressurized Irrigation Techniques; Food and Agriculture Organization of the United Nations.
26. **Raymond Hunt Jr., E., Li Li, Friedman, J.M., Gaiser, P.W., Twarog, E., Cosh, M.H. 2018.** Incorporation of StemWater Content into Vegetation Optical Depth for Crops and Woodlands. *Remote Sens.*, 10, 273; <https://doi:10.3390/rs10020273>
27. **Richard Seager, Allison Hooks, Park Williams, A., Benjamin Cook, Jennifer Nakamura, Naomi Henderson 2015.** Climatology, variability and trends in United States vapor pressure deficit, an important fire-related meteorological quantity. *Journal of Applied Meteorology and Climatology*. 54, 1121-1141. <https://doi.org/10.1175/JAMC-D-14-0321.1>
28. **Rodell, M., Coauthors, J. 2004.** The global land data assimilation system. *Bull. Amer. Meteor. Soc.*, 85, 381–394.
29. **Roth, L., Aasen, H., Walter, A., Liebisch, F. 2018.** Extracting leaf area index using viewing geometry effects – a new perspective on high-resolution unmanned aerial system photography. *ISPRS Journal of Photogrammetry and Remote Sensing* 141: 161–175.
30. **Running, S.W, Gower, S.T. 1991.** Forest-BGC, a general model of forest ecosystem processes for regional applications II. Dynamic carbon allocation and nitrogen budgets. *Tree Physiol.* 9:147–160.
31. **Running, S.W, Nemani, R.R. 1991.** Regional hydrologic and carbon balance responses of forests resulting from potential climate change. *Clim. Change*. 19:349–368.
32. **SAITO, K., OGAWA, S., AIHARA, M., OTOWA, K. 2001.** Estimats of LAI for forest management in Okutama. The 22nd Asian Conference on Remote Sensing, 5-9 November 2001, Singapore.
33. **Tucker, C.J. 1980.** A Spectral method for determining the percentage green Herbage material clipped samples. *Remote Sensing of Environment* 9(2): 175–181.

34. **Turner, D.P., Cohen, W.B., Kennedy, R.E., Fassnacht, K.S., Briggs, J.M. 1999.** Relationships between leaf area index, fapar, and net primary production of terrestrial ecosystems. *Remote Sens. Environ.* 70, 52–68.
35. USGS. 2020. Earth Explorer. <http://earthexplorer.usgs.gov/> (accessed 05.04.15).
36. USGS. 2021. Earth Explorer. <http://earthexplorer.usgs.gov/> (accessed 05.04.15).
37. **Voogt, J. A., Oke, T.R. 2003.** Thermal remote sensing of urban climates. *Remote Sens. Environ.* 86, 370–384.
38. **Wang, L., Hunt, E.R. Jr., Qu, J.J., Hao, X., Daughtry, C.S.T. 2013.** Remote sensing of fuel moisture content from ratios of narrow-band vegetation water and drymatter indices. *Remote Sens Environ.* 129:103–10.
39. **Yan, H., Wang, S.Q., Billesbach, D., Oechel, W., Zhang, J.H., Meyers, T., Martin, T.A., Matamala, R., Baldocchi, D., Bohrer, G. 2012.** Global estimation of evapotranspiration using a leaf area index-based surface energy and water balance model. *Remote Sens. Environ.* 124, 581–595.
40. **Zhang, F., Zhou, G. 2015.** Estimation of canopy water content by means of hyperspectral indices based on drought stress gradient experiments of maize in the North Plain China. *Remote Sens.* 7:15203–23.
41. **Zhang, L., Zhou, Z., Zhang, G., Meng, Y., Chen, B., Wang, Y. 2012.** Monitoring the leaf water content and specific leaf weight of cotton (*Gossypium hirsutum* L.) in saline soil using leaf spectral reflectance. *Europ J Agron.* 41:103–17.
42. **Zhou, S., Duursma, R.A., Medlyn, B.E., Kelly, J.W.G, Prentice, I.C. 2013.** How should we model plant responses to drought? An analysis of stomatal and non-stomatal responses to water stress. *Agric For Meteorol.* 182:204–214.
<https://doi.org/doi:10.1016/j.agrformet.2013.05.009>
43. **Zhou, W., Huang, G., Cadenasso, M.L. 2011.** Does spatial configuration matter? Understanding the effects of land cover pattern on land surface temperature in urban landscapes. *Landscape Urban Plan.* 102, 54–63.
<https://doi.org/10.1016/j.landurbplan.2011.03.009>

1/8/2022